Evolution of the Triplet Excited State in Pt^{II} Perylenediimides

Evgeny O. Danilov,[†] Aaron A. Rachford,[‡] Sébastien Goeb,[‡] and Felix N. Castellano*[,‡]

Department of Chemistry and Center for Photochemical Sciences, and Ohio Laboratory for Kinetic Spectrometry, Bowling Green State University, Bowling Green, Ohio 43403

Received: February 11, 2009; Revised Manuscript Received: March 20, 2009

Here, we present the ultrafast dynamics of a series of metal complexes developed to permit access to the perylenediimide (PDI) triplet manifold that preserves the desirable colorfastness and visible light-absorption properties associated with these dyes. To this end, three Pt^{II} complexes each bearing two PDI moieties tethered to the metal center through acetylide linkages emanating from one of the PDI bay positions have been thoroughly examined by static spectroscopic methods, electrochemistry, laser flash photolysis, and ultrafast transient absorption spectrometry. Upon ligation to the Pt^{II} center, the bright singlet-state fluorescence (Φ = 0.91, τ = 4.53 ns) of the free PDI−CCH chromophore is quantitatively quenched, and no long wavelength photoluminescence is observed from any of the Pt^{II}−PDI complexes in deaerated solutions. Ultrafast transient measurements reveal that upon ligation of PDI−CCH to the Pt^{II} center, picosecond intersystem crossing (τ = 2−4 ps) from the ^{1}PDI excited state is followed by vibrational cooling (τ = 12−19 ps) of the hot ^{3}PDI excited state, whereas only singlet-state dynamics, including stimulated emission, were observed in the "free" PDI−CCH moiety. In each of the Pt−PDI chromophores, quantitatively similar transient absorption difference spectra were obtained; the only distinguishing characteristic is in their single-exponential lifetimes (τ = 246 ns, 1.0 μs, and 710 ns). These long-lived ^{3}PDI excited states are clearly poised for bimolecular electron and energy transfer schemes. In the present case, the latter is demonstrated through bimolecular sensitization of singlet oxygen phosphorescence at ∼1270 nm in aerated dichloromethane solutions, producing reasonable $^1O_2$ quantum yields (Φ_Δ = 0.40−0.55) across this series of molecules.

Introduction

Perylenediimides (PDIs) continue to be incorporated into a variety of photofunctional materials.[1,2] In addition to their desirable visible light-harvesting and impressive fluorescence properties, PDIs have established niche applications in chemical sensing,[3,4] organic field-effect transistors,[5,6] light-emitting diodes,[7] and photovoltaics (PVs).[6,8] Given recent reports highlighting how polymeric PV performance is enhanced by utilizing long-lived triplet excited states in the photoinduced charge separation step,[9,10] access to the PDI triplet state clearly represents a desirable goal for solar energy conversion using these molecules. Despite recent attempts,[11] the PDI triplet state remains accessible only through bimolecular sensitization[12] or in sophisticated molecular architectures involving a cascade of nonradiative steps.[2,13–15] Last year, we designed molecules **1**−**3** in an effort to efficiently generate the triplet state of PDI following photoexcitation in three distinct Pt^{II} 16-electron square planar structures.[16] The platinum−acetylide motif was selected as this combination is known to induce strong spin−orbit coupling facilitating rapid (k_{isc} > 10^{11} s^{-1}) singlet → triplet intersystem crossing in the appended organic chromophore.[10,17] Structures **2** and **3** examine the influence of *cis*- vs *trans*-PDI−acetylide ligation, whereas **1**, which inherently possesses a more complex electronic structure, assesses the consequence of positioning a triplet charge transfer (^{3}CT) excited state energetically proximate to the PDI triplet. Our initial investigation led to the assignment of a lowest energy ^{3}PDI excited state in all three Pt^{II} chromophores. As we relied solely on nanosecond laser flash photolysis experiments, no dynamic information was available regarding the evolution of the initial Franck−Condon state.[16]

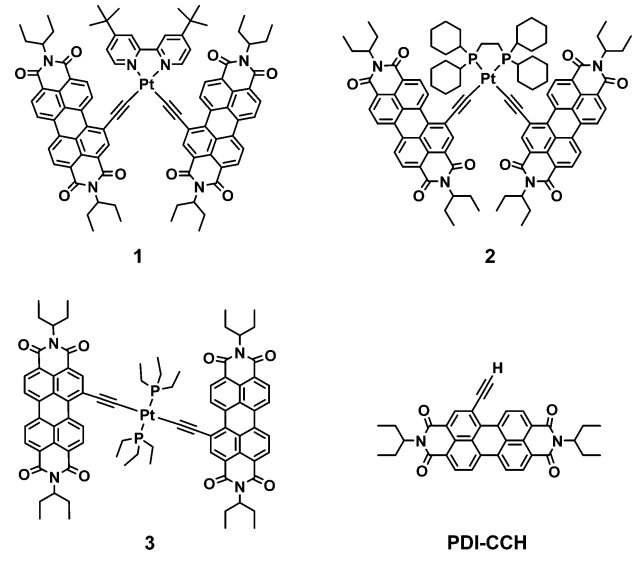

This present contribution is an expansion of our previous work[16] which now includes electrochemistry, sensitized singlet oxygen phosphorescence quantum yields, and ultrafast transient absorption spectrometry in an effort to more fully understand the triplet excited-state evolution and establish viable bimolecular photochemistry from these intrinsically interesting chromophores. The ^{3}PDI excited state is sufficiently long-lived

* To whom correspondence should be addressed. E-mail: castell@bgsu.edu.
† Department of Chemistry and Center for Photochemical Sciences.
‡ Ohio Laboratory for Kinetic Spectrometry.

10.1021/jp9012762 CCC: $40.75
Published on Web 04/17/2009

TABLE 1: Electrochemical and Photophysical Properties of 1−3 and PDI−CCH in CH_2Cl_2

compound	E_{ox} (V)[a,b]	E_{red} (V)[a]	λ_{abs} (nm)	Φ_Δ	τ_{ISC} (ps)	τ_{IVR} (ps)	τ_{3IL} (μs)
1	0.82	−1.14, −1.34, −2.05	573	0.40	2.25−2.6	10−13	0.246
2	0.84	−1.19, −1.44	570	0.55	3.8−4.9	18−19.2	1.0
3	0.85	−1.20, −1.40	570	0.54	4.1−4.26	13.8−16	0.710
PDI−CCH	−	−1.03, −1.24	529	−	−	−	−

[a] Potentials vs $Fc^{+/0}$. [b] Irreversible process.

(nanosecond to microsecond) to effectively produce singlet oxygen with modest quantum yields from all three Pt^{II}-containing structures (>40%). Here, we find that the previously assigned lowest ^{3}PDI excited state in **1**−**3** is generated on a picosecond time scale via intersystem crossing from the ^{1}PDI manifold. While compound **1** contains an energetically proximate ^{3}CT excited state, the presence of this state appears to only affect the excited-state decay of ^{3}PDI* and imparts no measurable influence on the time constant of intersystem crossing.

Experimental Section

General. All compounds investigated herein were available from our previous work.[16] Cyclic and differential pulse voltammetry experiments were performed in CH_2Cl_2 solutions with 0.15 M *n*-Bu_4NPF_6 ($TBAPF_6$) as supporting electrolyte at room temperature. A platinum disk working, platinum wire auxiliary, and Ag/AgCl (3 M NaCl) reference electrode were used for all electrochemical measurements. Fresh CH_2Cl_2 was of spectroscopic grade for all electrochemistry experiments, and $TBAPF_6$ was recrystallized from ethanol a minimum of three times. The solutions were thoroughly degassed with argon prior to each measurement. The ferrocenium/ferrocene couple ($FeCp_2^{+/0}$) was used as an internal reference (0.46 V vs Ag/AgCl). All voltammograms were recorded at room temperature with a Bioanalytical Systems Epsilon controller interfaced to a Pentium PC. Static UV−vis absorption spectra were measured with a Varian 50 Bio spectrophotometer or a Hewlett-Packard 8453 diode array spectrophotometer. Corrected steady-state luminescence spectra were obtained by a PTI Instruments spectrofluorimeter equipped with a Peltier cooled InGaAs detector using lock-in detection. This fluorimeter operates under the control of FeliX32 software from PTI. For $^1O_2$ emission sensitization experiments, a Melles Griot Series 74 He−Cd laser was used as the excitation source where the 442 nm output (38.2 mW) was directed into the PTI fluorimeter 90° to the detector. The laser power was measured with a Molectron Power Max 5200 power meter. All photophysical measurements were conducted at ambient temperature, 22 ± 2 °C, in spectroscopic grade CH_2Cl_2 in 1 cm^2 anaerobic quartz cells (Starna Cells), degassed by solvent-saturated high-purity argon for at least 35 min prior to the measurements and maintained under argon atmosphere throughout the experiments. Fluorescence lifetime measurements were obtained by time-correlated single-photon counting on an Edinburgh Analytical Instruments (FLSP 920) spectrofluorimeter equipped with a pulsed H_2 flashlamp (nF900). The instrument response function was collected using a dilute solution of Ludox at the detection wavelength. Reconvolution of the fluorescence decay and instrument response function was performed using the Edinburgh software in conjunction with lifetime fitting. Finally, the data was exported and plotted using Origin 8.0. Singlet fluorescence quantum yields of PDI−CCH in dichloromethane ($\eta = 1.424$) were determined relative to rhodamine B in water ($\Phi_{fl} = 0.41$; $\eta = 1.3387$) and are reported as an average of at least three measurements. Singlet oxygen quantum yield measurements were determined relative to perinaphthenone,[18] and reported values represent an average of at least three independent measurements.

Nanosecond Transient Absorption Spectrometry. Nanosecond transient absorption spectra were collected on a Proteus spectrometer (Ultrafast Systems) equipped with a 150 W Xe-arc lamp (Newport), a Chromex monochromator (Bruker Optics) equipped with two diffraction gratings blazed for visible and near-IR dispersion, respectively, and Si or InGaAs photodiode detectors (DET 10A and DET 10C, Thorlabs) optically coupled to the exit slit of the monochromator. Excitation at 450 nm with a power of 2.0 mJ/pulse from a computer-controlled Nd:YAG laser/OPO system from Opotek (Vibrant LD 355 II) operating at 10 Hz was directed to the sample with an optical absorbance of 0.4 at the excitation wavelength. The data consisting of a 128-shot average were analyzed by Origin 8.0 software.

Ultrafast Transient Absorption Spectrometry. Ultrafast transient absorption measurements were performed using the subpicosecond pump−probe UV−vis spectrometer described elsewhere.[19] Briefly, 1 mJ, 100 fs pulses at 800 nm at 1 kHz repetition rate were obtained from a Ti:Sapphire regenerative amplifier (Spectra Physics Hurricane). The output laser beam was split into pump and probe (85 and 8%). The pump beam was directed into a parametric amplifier (Spectra-Physics OPA-800C) to produce excitation pulses at 575 or 550 nm and then focused into the sample. The probe beam was passed through a computer-controlled optical delay (Newport MM4000 250 mm linear positioning stage) and then focused into a CaF_2 or sapphire crystal to generate the white light continuum. The white light was then overlapped with the pump beam in a 2 mm thick quartz sample cell and then coupled into a CCD detector (Ocean Optics S2000 UV−vis). Relative polarizations of the pump and probe beams were set at the magic angle. Data acquisition was controlled by in-house-developed National Instruments LabView software.

Results and Discussion

Electrochemistry. Cyclic voltammograms (CV) and differential pulse voltammograms (DPV) were obtained in deaerated dichloromethane with a Ag/AgCl (3 M NaCl) reference electrode, and all values are referenced to a Fc^+/Fc^0 internal standard. The electrochemical and photophysical properties are summarized in Table 1. Compound **1** displays two reversible ($i_{pc}/i_{pa} \sim 1$) PDI-based one-electron reductions at −1.14 and −1.34 V and a dbbpy-based reduction at −2.05 V, while the irreversible HOMO (likely composed of Pt^{II} and PDI−acetylide character) oxidation occurs at 0.82 V as a peak in the CV experiment. In the DPV experiment this oxidation occurs at a peak potential of 0.84 V, in close agreement with the CV experiment. Complex **2** displays similar PDI-based reductions at −1.19 and −1.44 V, while those of **3** appear at −1.20 and −1.40 V. Structures **2** and **3** also give similar HOMO oxidation potentials at 0.84 and 0.85 V, respectively. DPV was performed on **3**, producing a peak oxidation potential of 0.88 V which is again in reasonable agreement with the CV data. The corre-

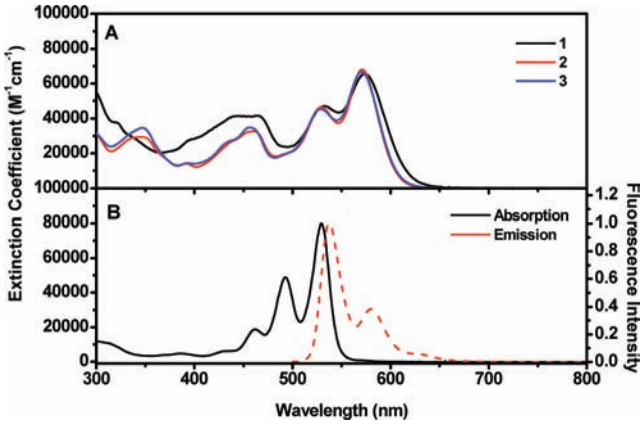

Figure 1. (A) Absorption spectra of **1**−**3**. (B) Absorption and fluorescence spectra of PDI−CCH. All spectra were collected in CH_2Cl_2.

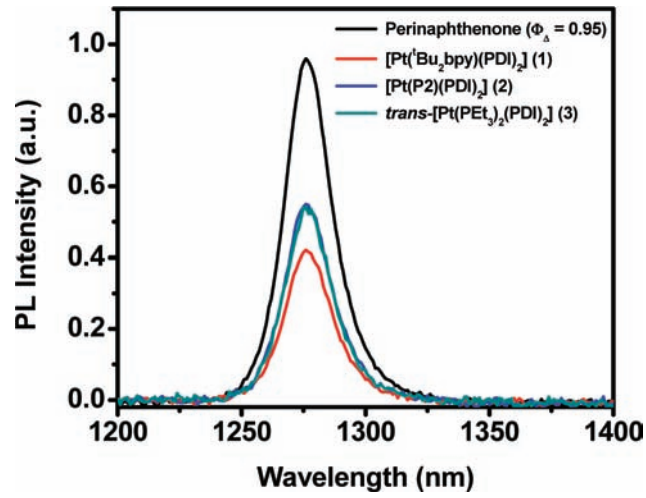

Figure 2. Sensitization of $^1O_2$ phosphorescence by **1**−**3** relative to perinaphthenone in aerated dichloromethane solutions.

sponding DPV experiment was not performed on **2** due to limited purified sample, but based upon the other two complexes we believe that the irreversible oxidation potential is not anticipated to be markedly displaced from the CV data. Although shifted to slightly more negative potentials, the PDI-based reduction potentials are within the expected range as PDI−CCH demonstrates two reversible one-electron reductions at −1.03 and −1.24 V vs Fc^+/Fc^0. These values are within the expected range for the first and second reduction of PDI.[11,20–22]

Static Absorption and Photoluminescence. Figure 1 presents the absorption spectra of **1**−**3** as well as the absorption and emission spectra of PDI−CCH measured in dichloromethane. The absorption spectra of all three Pt^{II} complexes are dominated by the $\pi-\pi^*$ transitions of the PDI moiety with maxima between 570 and 573 nm ($\epsilon \approx 65500-68000$ M^{-1} cm^{-1}). These absorptions are significantly red-shifted relative to that of the PDI−CCH chromophore (529 nm, $\epsilon = 80\,000$ M^{-1} cm^{-1}), as is typically observed when a conjugated terminal acetylene produces the corresponding Pt^{II}−acetylide chromophore.[16,17,23,24] Surprisingly, the extinction coefficients of **1**−**3** are not double that of the PDI−CCH; however, integration of each absorption spectrum yielded the expected 2:1 ratio (based on number of PDIs) for complexes **2** and **3** relative to PDI−CCH. A significant increase in extinction coefficient is also observed for **1** in the 375−500 nm region which results from the overlapping CT transition ($Pt^{II} \rightarrow$ dbbpy), thereby rendering a greater than 2:1 integrated absorption ratio relative to PDI−CCH. This agrees well with the electrochemistry of **1** (see above) as the irreversible one-electron HOMO oxidation (0.82 V) and bpy-based reduction (−2.05 V) energy difference predicts an additional absorption of MLCT parentage centered at ∼ 430 nm. PDI−CCH exhibits strong fluorescence (Φ = 0.91) centered at 537 nm with a lifetime of 4.53 ns.[16] Upon ligation via an acetylide bridge in the bay region to Pt^{II}, the fluorescence is quantitatively quenched in **1**−**3**, and no corresponding phosphorescence is detected in the visible or near-IR under degassed conditions at room temperature and 77 K. Production of nonluminescent triplet excited states has also been demonstrated in related Pt^{II}−CC−perylene chromophores.[24]

Singlet Oxygen Sensitization. Complexes **1**−**3** are nonemissive throughout the visible and NIR both at room temperature and 77 K. However, the long-lived excited states determined by nanosecond transient absorption (see below) provide opportunities for diffusive excited-state bimolecular electron and energy transfer reactions. The latter is effectively demonstrated as aerated dichloromethane solutions of each chromophore readily sensitize the distinctive phosphorescence of singlet oxygen ($^1O_2$) at ∼1270 nm upon excitation at 442 nm (Figure 2). Compounds **1**−**3** sensitize $^1O_2$ with reasonable quantum efficiencies, $\Phi_\Delta = 0.40$, 0.55, and 0.54, respectively. Of course, the sensitization of $^1O_2$ does not occur under the same conditions when the solutions are thoroughly degassed with either argon or nitrogen. $^1O_2$ being readily sensitized in good yield provides indirect evidence for a lowest triplet excited-state assignment for **1**−**3**. The present Φ_Δ values are in good agreement with those obtained in a related PDI system.[25] We note that geometry of the two PDI moieties does not appear to affect Φ_Δ; however, the excited-state lifetime of each respective chromophore is the dominant factor in determining Φ_Δ, increasing with increasing lifetime. The lack of photoluminescence emanating from any of the three chromophores also indicates that the nature of the excited state should be similar in all three instances.

Nanosecond Transient Absorption Spectroscopy. The nanosecond transient absorption spectra have been presented previously; however, for completeness we will reiterate these results here for a more complete presentation. The transient absorption difference spectra of **1**−**3** at selected delay times following 450 ± 2 nm pulsed laser excitation in CH_2Cl_2 at room temperature are presented in Figure 3; the single-exponential lifetimes measured in each case are indicated. Select single-wavelength kinetic traces and their respective fits with residuals are provided as insets in each panel. All major features of the three difference spectra agree remarkably well with each other. The major visible absorption features measured in all three complexes are qualitatively similar and red-shifted relative to bimolecular triplet-state sensitization experiments performed on PDI−CCH using thioxanthone as the sensitizer.[12,16] Taken together, the experimental data support the conclusion that a long lifetime PDI-localized triplet state is readily produced in **1**−**3**.

The transient absorption spectrum of **1** (Figure 3A) does not exhibit features typical of the ^{3}CT excited state of Pt^{II} diimine chromophores.[17,23,24] The difference spectrum in Figure 3A reveals an intense excited-state absorption at 495 nm and ground-state bleach near 575 nm followed by a broad, less intense absorption between 620 and 880 nm and excited-state absorption centered at 1080 nm. These spectral features do not coincide with characteristic PDI singlet-state transient absorptions (see below) or the associated radical cations or anions.[26–31] The excited-state lifetime of **1** as ascertained by transient

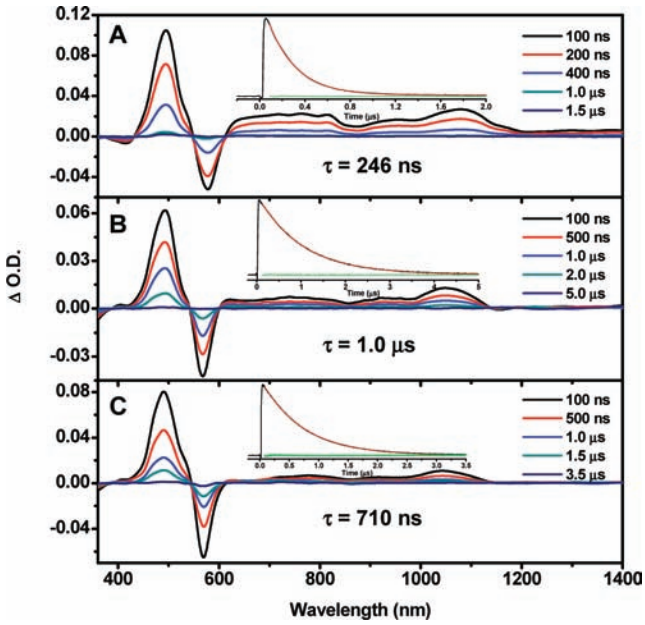

Figure 3. Nanosecond transient absorption difference spectra of **1** (A), **2** (B), and **3** (C). All transients were collected in deaerated CH_2Cl_2 at room temperature with $\lambda_{ex} = 450$ nm (2.5−3 mJ/pulse). Single-wavelength traces ($\lambda_{obs} = 490$ nm) with monoexponential fits (red) and residual plots (green) are displayed as insets in each panel. Single-exponential decay times are indicated within each panel.

absorption kinetics is 246 ns, consistent with the anticipated PDI-localized triplet-state parentage.

The corresponding *cis*-disposed phosphine model complex **2** lacking CT excited states exhibits a transient absorption spectrum nearly identical to that of **1**, Figure 3B. The most disparate difference between **1** and **2** is that the excited-state lifetime is extended to 1.0 μs in **2**. This increase in lifetime may be accounted for by the lack of a low-lying ^{3}CT state in **2**, the presence of which may facilitate more efficient excited-state deactivation in **1**. To exclude the possibility of electronic coupling effects between neighboring PDI moieties in **1** and **2**, the corresponding *trans*-disposed model complex **3** was synthesized. Importantly, no quantitative changes occur in the position, shape, relative intensities, and number of transitions in the ground-state (Figure 1A) or transient absorption difference spectra (Figure 3C). This observation readily excludes the possibility of intramolecular interactions from neighboring PDI units. Interestingly, the excited-state lifetime of **3** ($\tau = 710$ ns) lies between that of **1** and **2**, which implies that stereochemistry and the nature of the coordinated ligands profoundly influence the excited-state dynamics in these PDI−acetylide chromophores. This remains a point of interest for future investigation.

Ultrafast Transient Absorption (UFTA) Spectrometry. The transient absorption difference spectra at select delay times of PDI−CCH following excitation by 535 nm laser pulses are shown in Figure 4. The negative ΔOD signal at 535 with a shoulder at 540 nm and a negative signal at 586 nm at the prepulse delay time (black line) are due to the scattered excitation light (535 nm) and non-time-resolved fluorescence. The symmetric negative transient signal at positive delay times represents a mirror-imaged absorption and emission spectrum, corresponding to ground-state bleaching and stimulated emission. Positive transient absorption signals with maxima at 360 and 725 nm are observed within the spectral range of the experimental system. These features are attributed to excited-state absorption of the lowest energy singlet excited state of

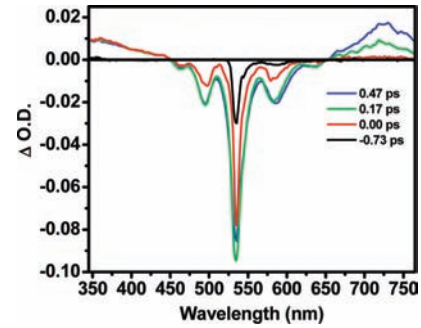

Figure 4. Picosecond transient absorption spectra of PDI−CCH in CH_2Cl_2 at selected delay times.

PDI−CCH and are in excellent agreement with features observed in other PDI-based systems exhibiting ^{1}PDI excited states.[2,11,20,32,33] Importantly, the signal does not decay significantly within the experimental time window (1.6 ns) as the singlet lifetime as determined from fluorescence lifetime measurements is 4.53 ns.

Picosecond transient absorption spectra of **1** at select delay times along with single-wavelength decays (507 and 750 nm) and exponential fits are provided in Figure 5. At early delay times (Figure 5A, upper panel) the prompt transient absorption spectrum is characterized by two ground-state bleaches near 530 and 580 nm and a broad featureless excited-state absorption at ∼750 nm. Taken together, these transient absorption features are in excellent agreement with that of a PDI singlet excited state and are in good agreement with features present in PDI−CCH though being red-shifted in energy as are the ground-state absorptions (Figure 1). Here, the mirror image stimulated emission observed for PDI−CCH is not observed in **1** as singlet fluorescence is quantitatively quenched for all three Pt−PDI chromophores by a process faster than the singlet-state radiative rate constant, $k_r = 2.0 \times 10^8$ s^{-1}. At longer delay times (Figure 5A, lower panel), the spectral features undergo significant changes such that a new excited-state absorption is established near ∼500 nm. Accordingly, the two bleaches have now completely changed shape so that the ground-state bleach centered at 530 nm appears simply as a shoulder and the bleach at 580 nm has lost considerable intensity. At the same time the excited-state absorption at ∼750 nm is also depleted of most of its original intensity. These significant time-evolved changes in the transient absorption difference spectrum likely indicate changes in the electronic nature of the excited state. In fact, the 1.6 ns time-delayed spectra in all cases are in excellent agreement with that of the prompt nanosecond transient absorption difference spectra assigned to the ^{3}PDI excited state as discussed earlier.[16] Hence, the initial and final ultrafast transient absorption spectra are assigned as the ^{1}PDI and ^{3}PDI excited states, respectively.

Concomitant with these spectral changes, single-wavelength decays and fitted time constants provide insight into the kinetics of surface crossing from the ^{1}PDI excited state to the ^{3}PDI excited state. The 507 nm decay must be fit to a sum of three single-exponential decays (Figure 5B, upper panel). The shortest time component represents the in-pulse formation of the ^{1}PDI excited state which is required for kinetic modeling at this particular wavelength. The kinetic trace contains two additional time components of $\tau_2 = 2.24$ ps and $\tau_3 = 10.2$ ps. These values are in excellent agreement with the time constants revealed by fitting the decay at 750 nm (Figure 5B, lower panel). Two time constants of $\tau = 2.58$ and 13.3 ps were extracted by fitting the data to a sum of two single-exponential decays. Intersystem

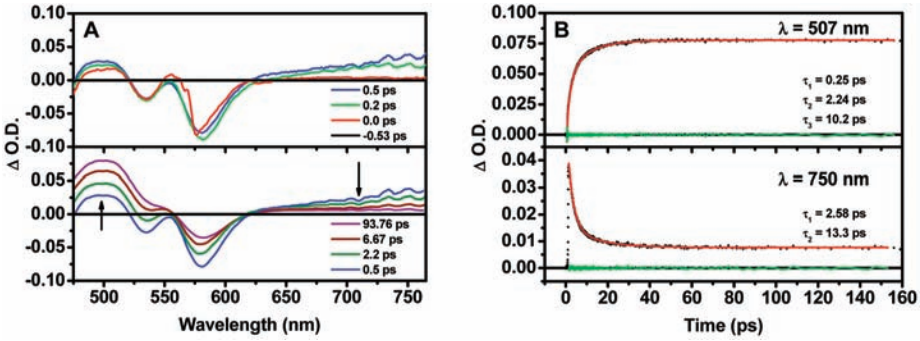

Figure 5. Picosecond transient absorption spectra of **1** in CH_2Cl_2 at selected delay times (A) and single-wavelength kinetic traces (black) with corresponding fits (red) superimposed (B). Residual plots (green) are presented for both fits.

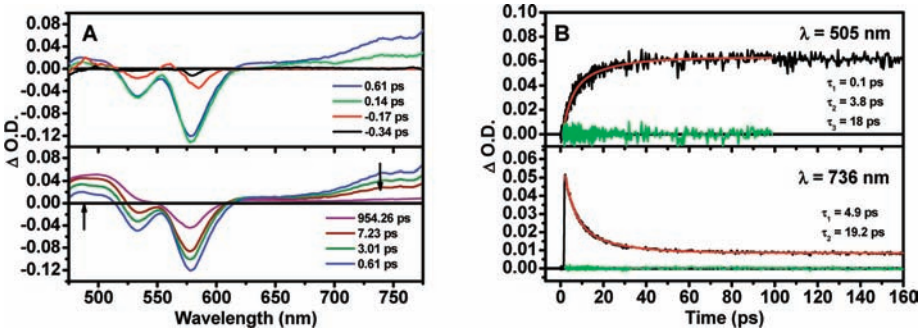

Figure 6. Picosecond transient absorption spectra of **2** in CH_2Cl_2 at selected delay times (A) and single-wavelength kinetic traces (black) with corresponding fits (red) superimposed (B). Residual plots (green) are presented for both fits.

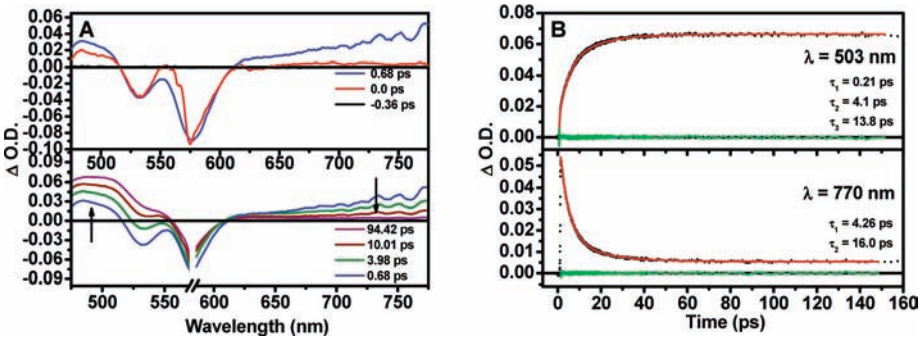

Figure 7. Picosecond transient absorption spectra of **3** in CH_2Cl_2 at selected delay times (A) and single-wavelength kinetic traces (black) with corresponding fits (red) superimposed (B). Residual plots (green) are presented for both fits.

crossing with time constants of 2.25−2.60 ps followed by thermalization of the triplet state with time constants ranging between 10 and 13 ps is not unexpected for aromatic chromophores tethered to Pt^{II} via an acetylide linkage. Similar kinetic processes have been observed and reported by us for a series of Pt−CC−pyrene complexes.[17] Following a 575 nm 100 fs excitation pulse, the promptly formed ^{1}PDI excited state of **1** undergoes intersystem crossing with a time constant of 2.25−2.58 ps forming vibrationally hot ^{3}PDI, which then thermalizes with a time constant between 10 and 13 ps, producing the lowest energy ^{3}PDI excited state.

Picosecond transient absorption difference spectra of **2** at select delay times along with single-wavelength decays (505 and 736 nm) and multicomponent exponential fits are provided in Figure 6. Similar to **1**, the early transient difference spectra (Figure 6A, upper panel) reveal features attributed to the ^{1}PDI excited state and a complete absence of stimulated emission. Longer delay times (Figure 6A, lower panel) depict changes also in agreement with **1** such that ISC occurs to generate vibrationally hot ^{3}PDI which then cools, producing the relaxed ^{3}PDI excited state. Kinetic analysis at 505 nm (Figure 6B, upper panel) again illustrates the in-pulse formation of the ^{1}PDI excited state, an ISC time constant of 3.8 ps which is followed by vibrational cooling with a time constant of 18 ps. Analysis of the 736 nm wavelength data is in reasonable agreement with the 505 nm data, yielding a 4.9 ps ISC time constant along with a 19.2 ps thermalization time constant.

The ultrafast transient absorption spectroscopy of **3** (Figure 7) also yields similar results, although larger scattering of the excitation light occurred, changing the shape of the transient difference spectra near 575 nm. Nevertheless, this model compound displayed the same salient spectroscopic features as **1** and **2** (Figures 5 and 6, respectively). Prompt formation of ^{1}PDI on short time scales (Figure 7A, upper panel) is followed by ISC (τ = 4.1−4.26 ps, Figure 7B) and vibrational cooling of the ^{3}PDI excited state on longer time scales (Figure 7A, lower panel, and Figure 7B) with τ = 13.8−16 ps. All of the spectroscopic and electrochemical data obtained in the present study are collected in Table 1.

Fast ISC with $k \sim 2-5 \times 10^{11}$ s^{-1} is not surprising in compounds containing Pt^{II} because of its large spin−orbit coupling constant. However, our previous work also demon-

strated markedly accelerated ISC rates (more than 20 times) when a bipyridine ligand was introduced into Pt−C≡C−pyrene structures producing energetically proximate charge transfer excited states.[17] Dissimilar to those results, the ISC rate in compound **1** containing a bipyridine ligand only displays a modest increase from $\sim 2.5 \times 10^{11}$ to $\sim 5 \times 10^{11}$ s^{-1} relative to the other Pt^{II} structures. This observation can be rationalized taking into account the energies of states involved in the energy migration/ISC process. From the crossing of the PDI−CCH absorption and singlet-state emission curves at 530 nm (Figure 1), the energy of the S_1 state can be estimated as close to 2.34 eV while the $\pi-\pi^*$ transition bands of largely PDI parentage in the Pt^{II} compounds are significantly broader and red-shifted to ~2.14 eV. On the other hand, the absorption maximum of the charge transfer transition is at 425 nm in Pt(dbbpy)-$(CC-Ph)_2$, a model compound of primarily Pt^{II}−bipyridine charge transfer character. The onset of its ^{3}CT emission at 500 nm places the energy of the ^{1}CT−^{3}CT states between 2.9 and 2.5 eV,[23] which are significantly higher than the singlet- and triplet-state intraligand energies in compounds **1**−**3**. A comparison of ground-state absorption spectra of the charge transfer compound **1** with the models **2** and **3** (Figure 1) also suggests that a contribution from the charge transfer states enhances absorption in the shorter wavelength range, between 360 and 500 nm. As a result, introduction of the higher energy charge transfer states into the singlet and triplet manifolds does not create a barrierless channel of energy transfer and does not accelerate ISC substantially. This is in direct contrast to the pyrenylacetylide CT chromophore previously investigated wherein the ^{3}CT level was nested between the ^{1}IL and ^{3}IL excited states, effectively accelerating the ISC/triplet energy migration process.[17] In the present case, having the CT levels positioned well above the ^{1}IL PDI transitions does not provide a viable pathway for enabling subpicosecond ISC in this class of molecules.

Conclusion

This report describes an electrochemical and kinetic spectroscopic investigation on the electronic nature of three fascinating Pt^{II}−acetylide chromophores. Through acetylide attachment of the PDI ligand to Pt^{II}, new chromophores are generated displaying broader absorptions that extend toward the lower energy portion of the solar spectrum. This ligation quantitatively quenches the ^{1}PDI excited state through increased spin−orbit coupling facilitated by the Pt^{II} center which also produces the long-lived ^{3}PDI excited state. Ultrafast transient absorption data illustrates that the Franck−Condon state initially undergoes intersystem crossing with a time constant of 2−4 ps followed by vibrational cooling of the hot triplet state with a time constant of 12−19 ps. There was no pronounced effect of accelerated ISC revealed in compound **1** containing CT states of bipyridine origin. This observation is consistent with the energy placement of the CT states well above the intraligand triplet excited states of PDI. The present work has demonstrated that the presence of the Pt^{II}−acetylide motif enables picosecond timescale intramolecular triplet sensitization providing ultrafast access to the ^{3}PDI manifold. Once formed, the long-lived ^{3}PDI excited state can effectively undergo diffusive excited-state reactions demonstrated here through bimolecular singlet oxygen sensitization. Harnessing these long-lived ^{3}PDI excited states for real-world applications now seems plausible.

Acknowledgment. This research was financially supported by the U.S. Air Force Office of Scientific Research (FA9550-05-1-0276) and the ACS-PRF (44138-AC3). Ultrafast transient absorption measurements were performed in the Ohio Laboratory for Kinetic Spectrometry.

References and Notes

(1) Wurthner, F. *Chem. Commun.* **2004**, 1564–1579.
(2) Wasielewski, M. R. *J. Org. Chem.* **2006**, *71*, 5051–5066.
(3) Zang, L.; Liu, R.; Holman, M. W.; Nguyen, K. T.; Adams, D. M. *J. Am. Chem. Soc.* **2002**, *124*, 10640–10641.
(4) Wang, W.; Zhou, H.-H.; Niu, S.; Li, A. D. Q. *J. Am. Chem. Soc.* **2003**, *125*, 5248–5249.
(5) Jones, B. A.; Ahrens, M. J.; Yoon, M.-H.; Facchetti, A.; Marks, T. J.; Wasielewski, M. R. *Angew. Chem., Int. Ed.* **2004**, *43*, 6363–6366.
(6) Zhan, X.; Tan, Z.; Domercq, B.; An, Z.; Zhang, X.; Barlow, S.; Li, Y.; Zhu, D.; Kippelen, B.; Marder, S. R. *J. Am. Chem. Soc.* **2007**, *129*, 7246–7247.
(7) Ego, C.; Marsitzky, D.; Becker, S.; Zhang, J.; Grimsdale, A. C.; Mullen, K.; MacKenzie, J. D.; Silva, C.; Friend, R. H. *J. Am. Chem. Soc.* **2003**, *125*, 437–443.
(8) Breeze, A. J.; Salomon, A.; Ginley, D. S.; Gregg, B. A.; Tilman, H.; Horhold, H.-H. *Appl. Phys. Lett.* **2002**, *81*, 3085–3087.
(9) Shao, Y.; Yang, Y. *Adv. Mater.* **2005**, *17*, 2841–2844.
(10) Guo, F.; Kim, Y.-G.; Reynolds, J. R.; Schanze, K. S. *Chem. Commun.* **2006**, 1887–1889.
(11) Weissman, H.; Shirman, E.; Ben-Moshe, T.; Cohen, R.; Leitus, G.; Shimon Linda, J. W.; Rybtchinski, B. *Inorg. Chem.* **2007**, *46*, 4790–4792.
(12) Ford, W. E.; Kamat, P. V. *J. Phys. Chem.* **1987**, *91*, 6373–6380.
(13) Kelley, R. F.; Shin, W. S.; Rybtchinski, B.; Sinks, L. E.; Wasielewski, M. R. *J. Am. Chem. Soc.* **2007**, *129*, 3173–3181.
(14) Prodi, A.; Chiorboli, C.; Scandola, F.; Lengo, E.; Alessio, E.; Dobrawa, R.; Wurthner, F. *J. Am. Chem. Soc.* **2005**, *127*, 1454–1462.
(15) Jimenez, A. J.; Spaenig, F.; Rodriguez-Morgade, M. S.; Ohkubo, K.; Fukuzumi, S.; Guldi, D. M.; Torres, T. *Org. Lett.* **2007**, *9*, 2481–2484.
(16) Rachford, A. A.; Goeb, S.; Castellano, F. N. *J. Am. Chem. Soc.* **2008**, *130*, 2766–2767.
(17) Danilov, E. O.; Pomestchenko, I. E.; Kinayyigit, S.; Gentili, P. L.; Hissler, M.; Ziessel, R.; Castellano, F. N. *J. Phys. Chem. A* **2005**, *109*, 2465–2471.
(18) Schmidt, R.; Tanielian, C.; Dunsbach, R.; Wolff, C. *J. Photochem. Photobiol., A* **1994**, *79*, 11–17.
(19) Gentili, P. L.; Danilov, E. O.; Ortica, F.; Rodgers, M. A. J.; Favaro, G. *Photochem. Photobiol. Sci.* **2004**, *3*, 883–891.
(20) Flors, C.; Oesterling, I.; Schnitzler, T.; Fron, E.; Scheitzer, G.; Sliwa, M.; Herrmann, A.; Auweraer, M. v. d.; Schryver, F. C. d.; Mullen, K.; Hofkens, J. *J. Phys. Chem. C* **2007**, *111*, 4861–4870.
(21) Ford, W. E.; Hiratsuka, H.; Kamant, P. V. *J. Phys. Chem.* **1989**, *93*, 6692–6696.
(22) Rybtchinski, B.; Sinks, L. E.; Wasielewski, M. R. *J. Phys. Chem. A* **2004**, *108*, 7497–7505.
(23) Hua, F.; Kinayyigit, S.; Rachford, A. A.; Shikhova, E. A.; Goeb, S.; Cable, J. R.; Adams, C. J.; Kirschbaum, K.; Pinkerton, A. A.; Castellano, F. N. *Inorg. Chem.* **2007**, *46*, 8771–8783.
(24) Rachford, A. A.; Goeb, S.; Ziessel, R.; Castellano, F. N. *Inorg. Chem.* **2008**, *47*, 4348–4355.
(25) Veldman, D.; Chopin, S. M. A.; Meskers, S. C. J.; Janssen, R. A. J. *J. Phys. Chem. A* **2008**, *112*, 8617–8632.
(26) Shibano, Y.; Umeyama, T.; Matano, Y.; Tkachenko, N. V.; Lemmetyinen, H.; Araki, Y.; Ito, O.; Imahori, H. *J. Phys. Chem. C* **2007**, *111*, 6133–6142.
(27) Shibano, Y.; Umeyama, T.; Matano, Y.; Tkachenko, N. V.; Lemmetyinen, H.; Imahori, H. *Org. Lett.* **2006**, *8*, 4425–4428.
(28) Chen, L. X.; Xiao, S.; Yu, L. *J. Phys. Chem. B* **2006**, *110*, 11730–11738.
(29) Ramos, A. M.; Beckers, E. H. A.; Offermans, T.; Meskers, S. C. J.; Janssen, R. A. J. *J. Phys. Chem. A* **2004**, *108*, 8201–8211.
(30) Karapire, C.; Timur, C.; Icli, S. *Dyes Pigments* **2003**, *56*, 135–143.
(31) van der Boom, T.; Hayes, R. T.; Zhao, Y.; Bushard, P. J.; Weiss, E. A.; Wasielewski, M. R. *J. Am. Chem. Soc.* **2002**, *124*, 9582–9590.
(32) Prathapan, S.; Yang, S. I.; Seth, J.; Miller, M. A.; Bocian, D. F.; Holten, D.; Lindsey, J. S. *J. Phys. Chem. B* **2001**, *105*, 8237–8248.
(33) Baffreau, J.; Leroy-Lhez, S.; Hudhomme, P.; Groeneveld, M. M.; van Stokkum, I. H. M.; Williams, R. M. *J. Phys. Chem. A* **2006**, *110*, 13123–13125.

JP9012762